

Electrochemical Evaluation of Si-Incorporated Diamond-Like Carbon (DLC) Coatings Deposited on STS 316L and Ti Alloy for Biomedical Applications

† Jung-Gu Kim, Kwang-Ryeol Lee¹, Young-Sik Kim², and Woon-Suk Hwang³

*Department of Advanced Materials Engineering, Sungkyunkwan University
300 Chunchun-Dong, Jangan-Gu, Suwon 440-746, Korea*

¹*Future Technology Research Division, Korea Institute of Science and Technology
P.O. Box 131, Cheongryang, Sungbuk-Gu, Seoul 130-650, Korea*

²*School of Advanced Materials Engineering, Andong National University
388 Songchun, Andogn, 760-749, Korea*

³*School of Materials Science and Engineering, Inha University
Incheon, 402-751, Korea*

DLC coatings have been deposited onto substrate of STS 316L and Ti alloy using r.f. PACVD (plasma-assisted chemical vapor deposition) with a mixture of C₆H₆ and SiH₄ as the process gases. Corrosion performance of DLC coatings was investigated by electrochemical techniques (potentiodynamic polarization test and electrochemical impedance spectroscopy) and surface analysis (scanning electron microscopy). The electrolyte used in this test was a 0.89% NaCl solution of pH 7.4 at temperature 37°C. The porosity and protective efficiency of DLC coatings were obtained using potentiodynamic polarization test. Moreover, the delamination area and volume fraction of water uptake of DLC coatings as a function of immersion time were calculated using electrochemical impedance spectroscopy. This study provides the reliable and quantitative data for assessment of the effect of substrate on corrosion performance of Si-DLC coatings. The results showed that Si-DLC coating on Ti alloy could improve corrosion resistance more than that on STS 316L in the simulated body fluid environment. This could be attributed to the formation of a dense and low-porosity coating, which impedes the penetration of water and ions.

Keywords : DLC, corrosion, STS 316L, Ti alloy, coating

1. Introduction

The materials selected for biomedical applications come after years of research into the chemical and physical properties of a host of different candidate materials. Ideally, the material of choice will not only be biocompatible, but also have electrochemical properties that match the biomaterial being replaced bone of human. STS 316L and Ti alloy have several advantages such as superior biocompatibility and corrosion resistance.¹⁻³⁾ However, the overall reaction of the human body on an implant is a system property that includes many different aspects, such as surface chemistry, implant movement, biodegradation and surgical aspects. The highly corrosive environment of the human body restricts the materials to be used for implants.⁴⁾ High corrosion resistance is required for the

material to use in this corrosive environment.⁵⁾ Moreover, wear debris produced from movement of joints can lead to wear-corrosion causing biodegradation.⁶⁾ Recently, many researchers have focused on the development of advanced biomaterials to complement these drawbacks. DLC coatings are suitable materials for biomedical application. DLC coatings have been the subject of extensive investigation in recent years because of its potential of attaining highly desirable properties of technological interest.⁷⁾ Many authors have noted the potential of DLC coatings as a protective coating for biomedical applications. DLC coatings have been reported to have good biocompatibility, such as the absence of inflammatory responses in vitro when assessed by mouse peritoneal macrophages,⁸⁾ and the absence of histopathological changes in vivo when implanted in animal bone.⁹⁾ Furthermore, the unique combination of corrosion resistance, wear resistance, low friction, chemical inertness and electrical insulation make

† Corresponding author: kimjg@skku.ac.kr

DLC increasingly the preferred candidate for wear-resistant and protective coatings. However, it is difficult to obtain the coatings which exhibit good adhesion on substrates. Another authors have informed on the use of amorphous silicon intermediate layer to improve the adhesion of DLC coatings using r.f. PACVD method.¹⁰⁾

This study is focused on the evaluation of the electrochemical performance of Si-DLC coatings on STS 316L and Ti alloy with amorphous silicon intermediate layer prepared by r.f. PACVD using electrochemical techniques.

2. Experimental procedure

2.1 Coating deposition

Si-wafer, STS 316L and Ti alloy (Ti-6Al-4V) were used as substrate materials. Samples of 37 mm diameter were cut from a 2 mm thick sheet. DLC coatings were deposited on mirror-polished substrate. The sample surfaces were mechanically ground and polished using 2000-grit SiC and 0.3 μm diamond paste for the final step. After cleaning with methanol, the polished samples were stored under vacuum. A substrate was placed on the water-cooled cathode where 13.56 MHz r.f. power was delivered through the impedance-matching network. Before deposition, substrates were precleaned using argon ion for 15 min at bias voltage of -400 V and pressure of 9.975×10^{-3} Torr. The precursor gas was used as a mixture of C_6H_6 and silane (SiH_4) for the Si-DLC coatings. In r.f. PACVD method, the vacuum vessel is pumped by a rotary pump to a base pressure of approximately 2.0×10^{-5} Torr prior to deposition. A dense Si interlayer of thickness approximately 0.01 μm is deposited onto the substrate prior to DLC coating. The interlayer is deposited primarily to control and set up a residual stress gradient between the DLC coating and the substrate. A total coating thickness of about 1 μm was achieved in all cases. The film thickness was analyzed by alpha-step profilometer.

2.2 Surface analysis

The SEM investigations were used to examine the surface morphology of the coatings as well as the corroded surfaces of tested specimens. The SEM investigations took place with a voltage of 20 keV.

2.3 Electrochemical measurements

Potentiodynamic polarization test was determined with an EG&G Princeton Applied Research Model 273A potentiostat. Potentiodynamic polarization test was carried out in a 0.89% NaCl solution of pH 7.4 at temperature 37 °C which was thoroughly deaerated by bubbling high purity nitrogen gas for 30 min prior to the immersion of

the specimen and continuously purged during the test. This solution was simulated as a human body environment. The exposed coating area was 1 cm^2 . Reference and counter electrodes were used for a saturated calomel electrode (SCE) and a pure graphite, respectively. Prior to the beginning of the potentiodynamic polarization test, the specimens were kept in the solution for 6 h in order to establish the open-circuit potential (OCP). The potential of the electrode was swept at a rate of 0.166 mV/s from the initial potential of -250 mV versus E_{corr} to the final potential of 1500 mV_{SCE}. The porosity of DLC coating is estimated using electrochemical techniques. Porous coatings can not prevent the diffusion of aggressive agents through the coating, which lead to delamination of the coating. The porosity can be determined from the measured polarization resistance. Matthews et al.¹¹⁾ established an empirical equation to estimate the porosity (P) of the coatings:

$$(1)$$

where P was the total coating porosity, R_{pm} the polarization resistance of the substrate and R_{p} the measured polarization resistance of the coated steel system. ΔE_{corr} is the potential difference between the free corrosion potentials of the coated steel and the bare substrate, and β_{a} the anodic Tafel slope for the substrate. Also, protective efficiency (P_i) of the coating was determined from the polarization curve by Eq. (2):

$$(2)$$

where i_{corr} and i_{corr}^0 indicate that the corrosion current densities in the presence and absence of the coating, respectively.¹²⁾

Electrochemical impedance spectroscopy (EIS) has been frequently used as a non-destructive testing method for assessing the protective performance of coating. Moreover, EIS has been recognized as the powerful instrument to know the surface of the specimens.¹³⁾ EIS data were obtained by a Zahner IM6e system using commercial software (THALES) program for AC measurement. Impedance measurements were performed by applying a sinusoidal wave of 10 mV in amplitude to the working electrode at the frequency range from 10 kHz and 10 mHz. The impedance diagrams were interpreted on the basis of the equivalent circuit using THALES fitting program. EIS has been used to determine the amount of delamination and water uptake of coatings exposed to an electrolyte.

Thus, the extent of delamination area (A_d) and volume fraction of water uptake (V) could be determined from experimental values of pore resistance (R_{pore}) and coating capacitance (C_{coat}) obtained by the impedance diagrams on the basis of the equivalent circuit.¹⁴⁾

(3)

(4)

(5)

where R_{pore}^0 was characteristic value for the corrosion reaction at the solution/coating interface, d coating thickness, ρ the coating resistivity, $C_{coat}(t)$ the coating capacitance as a function of time (t) and $C_{coat}(0)$ the initial coating capacitance obtained from EIS data at initial exposure.

3. Results and discussion

3.1 Surface analysis

After the completion of potentiodynamic polarization

test, the morphology and corrosion features of each substrate and coated system were inspected by SEM and the resulting micrographs are shown in Fig. 1. Pitting was observed on both STS 316L and Ti alloy substrates in Figs. 1 (a) and (b). The surface morphology of Si-DLC coating on STS 316L showed some pitting areas, as indicated in Fig. 1(c). The surface morphology of Si-DLC coating on Ti alloy almost indicated no evidence of penetration of water and ions, as shown in Fig. 1(d). This clearly indicates that Si-DLC coating on Ti alloy have excellent corrosion resistance, and no damage has been observed. Moreover, it is also indicated that the penetration of water and ions of Si-DLC coating on Ti alloy is less than that of Si-DLC coating on STS 316L.

3.2 Electrochemical properties

Potentiodynamic polarization test was carried out in order to investigate the protective abilities of coating. Potentiodynamic polarization curves for Si-DLC coatings in the simulated body fluid environment are shown in Fig. 2. The measured corrosion potential (E_{corr}), corrosion current density (i_{corr}), porosity (P) and protective efficiency (P_i) are given in Table 1. The corrosion current density of 0.06486 nA/cm² for Si-DLC coating on STS 316L and that of 0.04099 nA/cm² for Si-DLC coating on Ti alloy were examined. It was seen that the passive region was

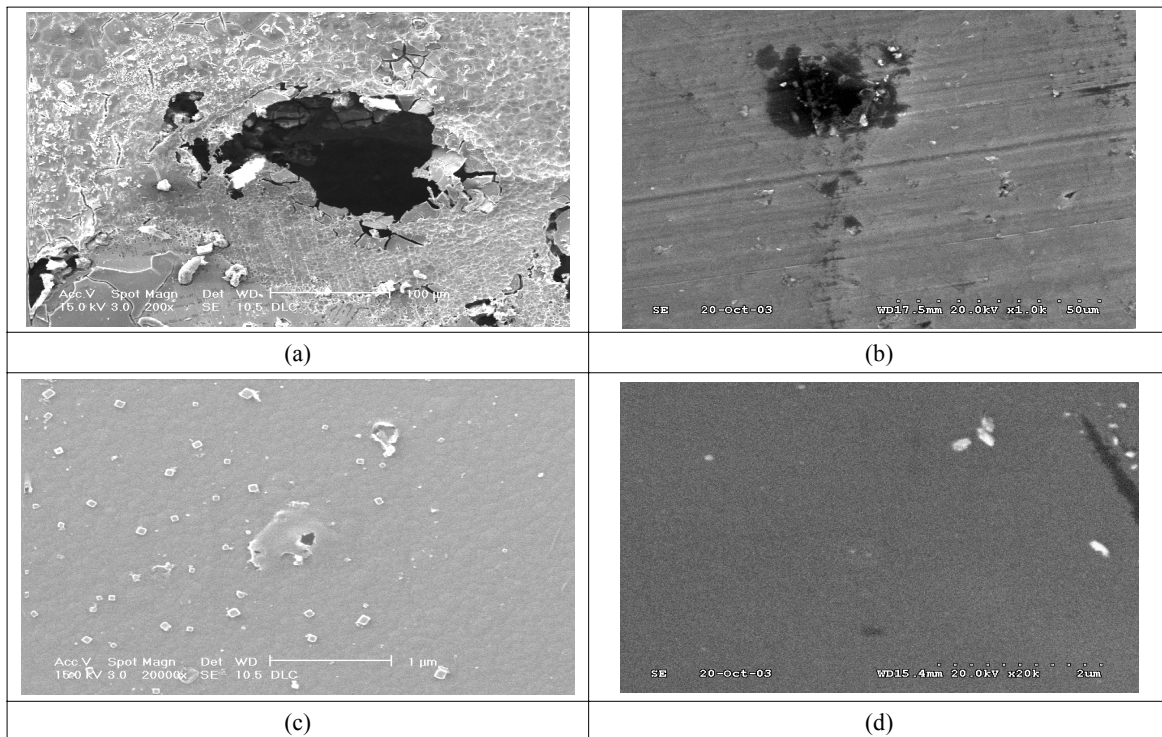


Fig. 1. SEM images showing surface morphologies of DLC coatings after polarization test; (a) STS 316L, (b) Ti alloy, (c) Si-DLC coating on STS 316L, (d) Si-DLC coating on Ti alloy

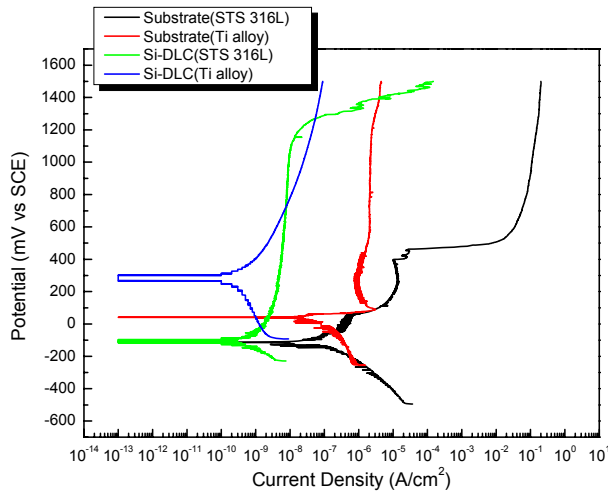


Fig. 2. Potentiodynamic polarization curves in deaerated 0. 89% NaCl solution at 37°C (pH=7.4);

formed on all the DLC coatings on STS 316L and Ti alloy. It means that Si-DLC coating on Ti alloy with fewer pores makes the substrate more passive than DLC coating on STS 316L with more pores. A combination of the equation of A. Matthews et al.¹¹⁾ and the electrochemical determinations gives the porosity of 0.00037 for Si-DLC on STS 316L and the porosity of 0.000043 for Si-DLC coating on Ti alloy. This pore can weaken the interfacial material and provide an easy fracture path for metallic ions release. It was shown that the porosity of DLC coating on Ti alloy was lower than that of DLC coating on STS 316 L. The lower the porosity, the denser the coating. Moreover, the lower the calculated porosity, the lower the corrosion current density. This means that the open channels of the substrate contacting with solution, which is often called pinhole, are significantly diminished. Therefore, the possi-

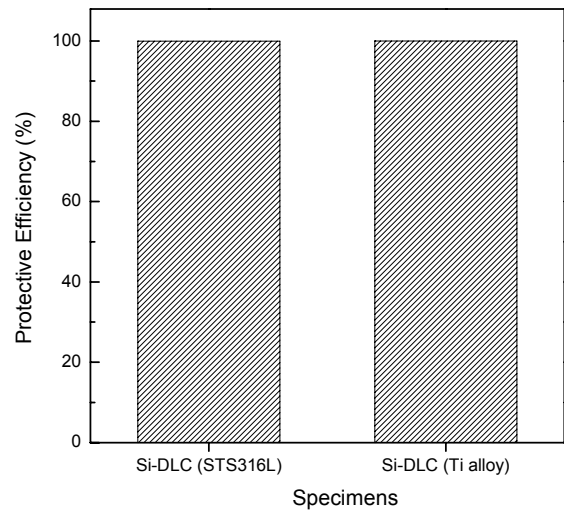


Fig. 3. Comparison of protective efficiency between DLC coating on STS 316L and DLC coating on Ti alloy

bility of a corrosive attack can be avoided and decreased.

Fig. 3 shows the protective efficiency calculated from corrosion current density described in Table 1.¹⁵⁾ The protective efficiency was 99.97 % and 99.98 % of Si-DLC coating on STS 316L and Ti alloy, respectively. It is shown that the protective efficiency of DLC coating on Ti alloy was higher than that of DLC coating on STS 316L. This is closely related to the corrosion protective ability and durability of coatings under conditions of applications. Thus, potentiodynamic polarization test were consistent with porosity measurement and protective efficiency measurement. If the coating had poor adhesion strength, the coating was extruded by the corrosion products and detached from substrate, and this made the corrosion products of substrate more severe. This means

Table 1. Results of potentiodynamic polarization tests; (a) DLC coating on STS 316 L, (b) DLC coating on Ti alloy (Ti-6Al-4V).¹⁵⁾

(a)

Specimen	E_{corr} (mV)	i_{corr} (nA/cm ²)	β_a (V/decade)	β_c (V/decade)	R_p ($\times 10^3 \Omega \cdot \text{cm}^2$)	Protective efficiency (%)	Porosity
Substrate(STS 316L)	-114.6	249.3	0.1285	0.1868	132.7	-	-
Si-DLC Bias voltage = -400V	-111.6	0.06486	0.3527	0.06077	347492.9	99.97	0.00037

(b)

Specimen	E_{corr} (mV)	i_{corr} (nA/cm ²)	β_a (V/decade)	β_c (V/decade)	R_p ($\times 10^3 \Omega \cdot \text{cm}^2$)	Protective efficiency (%)	Porosity
Substrate(Ti alloy)	-5.48	195.6	0.1142	0.4451	202.2	-	-
Si-DLC Bias voltage(-400V)	270.6	0.04099	0.2353	0.6027	1795037	99.98	0.0000043

Table 2. Result of electrochemical impedance spectroscopy measurements; (a) DLC coating on STS 316L, (b) DLC coating on Ti alloy (Ti-6Al-4V).¹⁶⁾

(a)

Exposure time		R _s (Ω cm ²)	CPE1		R _{pore} (×10 ³ Ω cm ²)	CPE2		R _{ct} (×10 ³ Ω cm ²)	A _d (*10 ⁻³)	V
			C _{coat} (×10 ⁻⁹ F/cm ²)	n (0-1)		C _{dl} (×10 ⁻⁹ F/cm ²)	n (0-1)			
120h	Substrate	32.96	46440	1	78.9	175200	1	252.2	-	-
	Si-DLC, (-400V)	700.7	20.8	0.9921	3.43	47.47	0.7483	2501	0.41	1.91
168h	Substrate	34.57	47980	1	76.53	169400	1	230.2	-	-
	Si-DLC, (-400V)	882.4	26.4	1	3.175	43	0.7375	3566	0.45	1.96
216h	Substrate	33.29	48210	1	73.4	174200	1	218.2	-	-
	Si-DLC, (-400V)	4.308	27.1	0.9602	2.9	47.05	0.5329	2062	0.48	1.97

(b)

Exposure time		R _s (Ω cm ²)	CPE1		R _{pore} (*10 ³ Ω cm ²)	CPE2		R _{ct} (*10 ³ Ω cm ²)	A _d (*10 ⁻⁴)	V
			C _{coat} (*10 ⁻⁹ F/cm ²)	n (0-1)		C _{dl} (×10 ⁻⁹ F/cm ²)	n (0-1)			
120h	Substrate	8334	20040	0.9944	33.28	29360	1	343.3	-	-
	Si-DLC, (-400V)	19470	0.759	0.9088	28799	13.05	1	324700	0.00049	0.15
168h	Substrate	1042	27530	1	39.52	33080	1	345.2	-	-
	Si-DLC, (-400V)	18540	0.816	0.9248	27789	13.89	1	298500	0.00051	1.17
216h	Substrate	1734	30470	1	44.61	34250	1	253.4	-	-
	Si-DLC, (-400V)	24540	0.897	0.8994	23569	14.72	1	299700	0.00060	1.19

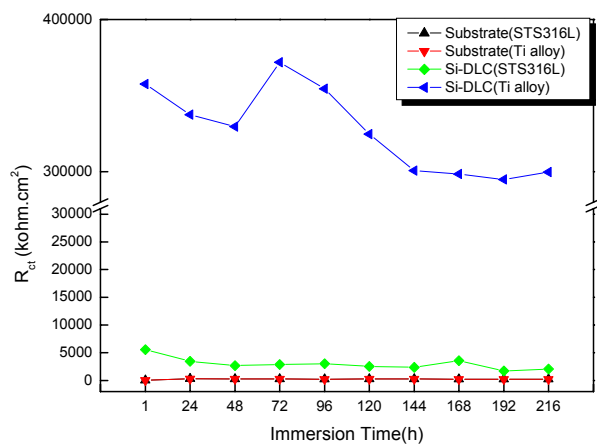


Fig. 4. Charge transfer resistance values as a function of immersion time between DLC coating on STS 316L and DLC coating on Ti alloy

that the detachment of coating makes the corrosive attack of interface between coating and substrate easier. That is, corrosion resistance is dependent on porosity, protective efficiency and adhesion strength of coating.

Interpretation of the EIS measurements is usually done by fitting the impedance data to an equivalent circuit, which is representative of the physical processes taking place in the system under investigation. According to the Table 2¹⁶⁾ and Fig. 4, the charge transfer resistance (R_{ct}) of DLC coating on Ti alloy was higher than that of Si-DLC coating on STS 316L. It is important that the high R_{ct} value indicates good corrosion resistance. Furthermore, it is also shown that Si-DLC coatings on Ti alloy have improved corrosion resistance more than that of DLC coating on STS 316L in corrosive environment.

Also, the results obtained from EIS measurements were usually used to monitor the change of delamination area (A_d) and volume fraction of water uptake (V). Figs. 5 and 6 show delamination area (A_d) and volume fraction of water uptake (V) of Si-DLC coatings on STS 316 L and Ti alloy, respectively. The delamination area of Si-DLC coating on STS 316L is much higher than that of Si-DLC coating on Ti alloy. Delamination area was affected by the volume fraction of water uptake through porous coating because penetration of water in coating lead to delami-

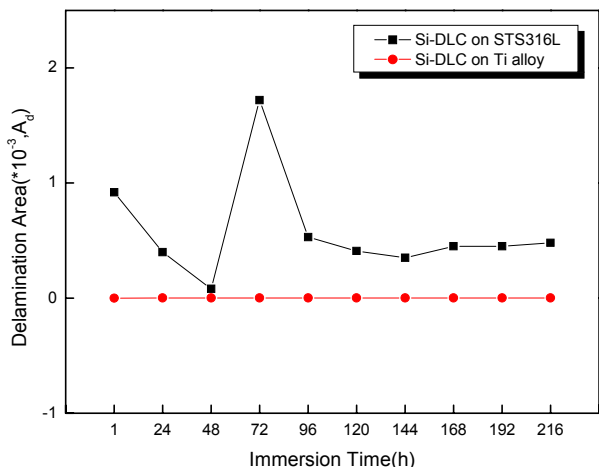


Fig. 5. Delamination area as a function of immersion time.

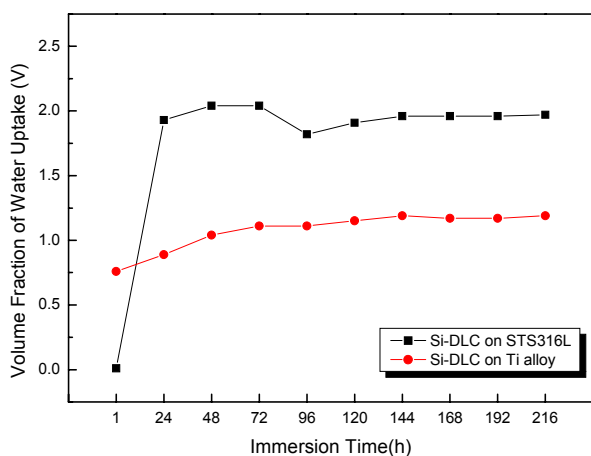


Fig. 6. Volume fraction of water uptake as a function of immersion time.

nation and blisters. It is seen that longer time of exposure leads to a continuous increase of the volume fraction of water uptake, as shown Fig. 6. Especially, the volume fraction of water uptake of Si-DLC coating on STS 316L tends to absorb more water due to the enhancement of diffusion mechanisms of active species through the coating. Consequently, delamination area and the volume fraction of water uptake of Si-DLC coating on Ti alloy are lower than those of Si-DLC coating on STS 316L, as shown in Figs. 5 and 6. This implies that Si-DLC coating on Ti alloy permeate less amount of water and ions than DLC coating on STS 316L.

The excellent agreement between the delamination area and the volume fraction of water uptake over the test period suggests that porosity is indeed strongly related to the coating delamination and the fraction of the substrate which is wetted by the electrolyte through defects.

4. Conclusions

(1) Si-DLC coating on Ti alloy (Ti-6Al-4V) showed lower corrosion current density, porosity and higher protective efficiency than that on STS 316L, indicating better corrosion resistance.

(2) Delamination area and the volume fraction of water uptake of Si-DLC coating on Ti alloy are lower than those of Si-DLC coating on STS 316L

(3) From the SEM analyses, the surface morphology of Si-DLC coating on Ti alloy indicated no evidence of pitting while that on STS 316L showed some pitting.

(4) The corrosion resistance of DLC coating on Ti alloy was better than that of DLC coating on STS 316L due to the low porosity.

Acknowledgments

This work was supported by Grant No. R11-2000-096-0000-0 from the Center of Excellency Program of the KOSEF, MOST.

References

1. K. Bordji, J. Jouzeau, D. Mainard, E. Payan, J. Delagoutte, and P. Netter, *Biomaterials*, **17**, 491 (1996).
2. H. Matsuno, A. Yokoyama, F. Watari, M. Uo, and T. Kawasaki, *Biomaterials*, **22**, 1253 (2001).
3. I. S. Lee, *Met. Mater. Int.*, **3**, 144 (1997).
4. R. Hauert, *Diam. Relat. Mater.*, **12**, 583 (2003).
5. Y. Hayashi and G. Nakayama, *Corrosion Science and Technology*, **1**, 491 (2002).
6. H. Kim and J. J. Lee, *J. Kor. Inst. Met. and Mater.*, **16**, 11 (2003).
7. P. Papakonstantinou, J. F. Zhao, P. Lemoine, E. T. McAdams, and J. A. McLaughlin, *Diam. Relat. Mater.*, **11**, 1074 (2002).
8. L. A. Thomson, F. C. Law, N. Rushton, and J. Franks, *Biomaterials*, **12**, 37 (1991).
9. D. P. Dowling, P. V. Kola, K. Donnelly, T. C. Kelly, K. Brumitt, L. Lloyd, R. Eloy, M. Therin, and N. Weill, *Diam. Relat. Mater.*, **6**, 390 (1997).
10. R. Butter, M. Allen, L. Chandra, A. H. Lettington, and N. Rushton, *Diam. Relat. Mater.*, **4**, 857 (1995).
11. B. Matthes, E. Brozeit, J. Aromaa, H. Ronkainen, S. P. Hannula, A. Leyland, and A. Matthews, *Surf. Coat. Technol.*, **49**, 489 (1991).
12. Y. J. Yu, J. G. Kim, S. H. Cho, and J. H. Boo, *Surf. Coat. Technol.*, **162**, 161 (2003).
13. T. H. Ha, D. K. Kim, J. H. Bae, H. G. Lee, and S. J. Lee, *Corrosion Science and Technology*, **1**, 444 (2002).
14. F. Mansfeld and C. H. Tsai, *Corrosion*, **49**, 727 (1993).
15. H. G. Kim, S. H. Ahn, and J. G. Kim, *Diam. Relat. Mater.*, **14**, 35 (2005).
16. H. G. Kim, S. H. Ahn, and J. G. Kim, *Thin Solid Films*, **475**, 291 (2005).